We are IntechOpen, the world's leading publisher of Open Access books Built by scientists, for scientists

4,800
Open access books available

122,000
International authors and editors

135M
Downloads

Our authors are among the

154
Countries delivered to

TOP 1%
most cited scientists

12.2%
Contributors from top 500 universities

WEB OF SCIENCE™

Selection of our books indexed in the Book Citation Index in Web of Science™ Core Collection (BKCI)

Interested in publishing with us?
Contact book.department@intechopen.com

Numbers displayed above are based on latest data collected.
For more information visit www.intechopen.com

2

Gaussian and Fourier Transform (GFT) Method and Screened Hartree-Fock Exchange Potential for First-principles Band Structure Calculations

Tomomi Shimazaki[1,2] and Yoshihiro Asai[1]
[1]*National Institute of Advanced Industrial Science and Technology (AIST),Umezono 1-1-1, Tsukuba Central 2, Tsukuba, Ibaraki 305-8568,*
[2]*Fracture and Reliability Research Institute (FRRI), Graduate School of Engineering, Tohoku University, 6-6-11-703 Aoba, Aramaki, Aoba-ku, Sendai, Miyagi 980-8579 Japan*

1. Introduction

The Gaussian and Fourier Transform (GFT) method is a first-principles quantum chemistry approach based on the Gaussian basis set, which can take into account the periodic boundary condition (PBC).(Shimazaki et al. 2009 a) The quantum chemistry method has mainly concentrated on isolated molecular systems even if target system becomes large such as DNA molecules and proteins, and the periodic nature does not appear. However, chemists have been recently paying much attention to bulk materials and surface, which cover electrochemical reaction, photoreaction, and catalytic behaviour on the metal or semiconductor surfaces. The periodic boundary condition in the first principles (*ab-initio*) approach is a strong mathematical tool for handling those systems. In addition to this, the momentum (k-space) description for the electronic structure helps us to understand essential physical and chemical phenomena on those systems. Therefore, it is an inevitable desire to extend the ordinary quantum chemistry method toward the periodic boundary condition. The crystal orbital method is a straight-forward extension for the purpose.(Hirata et al. 2010; Ladik 1999; Pisani et al. 1988) However, the crystal orbital method naturally faces a challenging problem to calculate the Hartree term due to the long-range behavior of the Coulomb potential. The method requires for infinite lattice sum calculations with respect to two electron integral terms, which intensively takes CPU costs even if some truncation is employed. Therefore, several computational techniques, such as sophisticated cutoff-criteria and the fast multi-pole method (FMM), have been developed to cope with the problem. (Delhalle et al. 1980; Kudin et al. 2000; Piani et al. 1980) In this chapter, we explain an efficient method using Fourier transform technique and auxiliary pane wave, whose description is suitable for the periodic boundary condition, to calculate the periodic Hartree term. Our method is based on the Gaussian basis set and the Fourier (GFT) transform method, thus we refer to our method as the GFT method. In the GFT method, the Hartree (Coulomb) potential is represented by auxiliary plane waves, whose coefficients are obtained by solving Poisson's equation based on the Fourier transform technique. However, the matrix element of the Hartree term is

determined in the real-space integration including Gaussian-based atomic orbtials and plane waves. We can employ a recursive relation to achieve the integration, as discussed later. Conversely, we can employ the effective core potential (ECP) instead of explicitly taking into account core electrons in the GFT method. This chapter will demonstrate several electronic band structures obtained from the GFT method to show the availability of our method for crystalline systems.

We try to develop the GFT method to become an extension of the ordinary quantum chemistry method, whereas our method employs the different integration algorithm for the Hartree term. Therefore, the various quantum chemistry techniques can be easily incorporated into the GFT method. In this chapter, we discuss the effect on the Hartree-Fock fraction term in the electronic structure calculation for solid-state materials. In first-principles calculations of crystalline and surface systems, local or semi-local density functional theory (DFT) is usually employed, but the use of the HF fraction can expand the possibility of DFT. The HF fraction is frequently adopted in the hybrid DFT functional, especially in the field of the quantum chemistry. It has been proved that the electronic structure description of the hybrid DFT method is superior compared with the local density (LDA) and generalized gradient approximations (GGA) in molecular systems. However, the hybrid DFT method is rarely adopted for crystalline and surface systems because of its larger computational cost.

When we discuss the hybrid DFT method in crystalline and surface systems, the concept of screening on the exchange term is imperative. The concept has been already taken into account in the HSE hybrid-DFT functional, which is proposed by Heyd et al. in 2003.(Heyd et al. 2003) On the other hand, the GW approximation handles the concept, whereas it is not in DFT framework.(Aryasetiawan et al. 1998; Hedin 1965) In the Coulomb hole plus screened exchange (COHSEX) approximation of the GW method, the screened exchange term is explicitly described. Thus, its importance has been recognized at early stage of first-principles calculations. However, the relationship between the hybrid-DFT method and the screening effect has not been paid attention so much. Recently, we propose a novel screened HF exchange potential, in which the inverse of the static dielectric constant represents the fraction of HF exchange term.(Shimazaki et al. 2010; Shimazaki et al. 2008; Shimazaki et al. 2009 b) The screened potential can be derived from a model dielectric function, which is discussed in Section III, and can give an interpretation how the screening effect behaves in semiconductors and metals. In addition, it will be helpful to present a physical explanation for the HF exchange term appeared in the hybrid-DFT method. In order to show the validity of our physical concept, we demonstrate several band structure calculations based on our screened HF exchange potential, and show that our concept on the screening effect is applicable to semiconductors. In this chapter, the screened HF exchange potential is incorporated with the GFT method, whereas it does not need to stick to the GFT method. The GFT method is based on the Gaussian-basis formalism, and therefore we can easily introduce the hybrid-DFT formalism for PBC calculations.

2. Gaussian and Fourier Transform (GFT) method

2.1 Crystal Orbital method

First we briefly review the crystal orbital method, which is a straight-forward extension of the quantum chemistry method to consider the periodic boundary condition.(Hirata et al. 2009; Hirata et al. 2010; Ladik 1999; Pisani et al. 1988; Shimazaki et al. 2009 c) The Bloch

function (crystal orbital) for solid-state material is obtained from the linear combination of atomic orbitals (LCAO) expansion as follows:

$$b_j^{\mathbf{k}}(\mathbf{r}) = \frac{1}{\sqrt{K}} \sum_{\alpha}^{M} \sum_{\mathbf{Q}}^{K} \exp(i\mathbf{k}\cdot\mathbf{Q}) d_{\alpha,j}(\mathbf{k}) \chi_{\alpha}^{\mathbf{Q}} \tag{1}$$

Where $\mathbf{Q}$ is the translation vector. The total number of cells is $K = K_1 K_2 K_3$, where K_1, K_2, and K_3 are the number of cells in the direction of each crystal axis, and $\mathbf{k}$ is the wave vector. $\chi_{\alpha}^{\mathbf{Q}} = \chi_{\alpha}(\mathbf{r} - \mathbf{Q} - \mathbf{r}_{\alpha})$ is the α-th atomic orbital (AO), whose center is displaced from the origin of the unit cell at $\mathbf{Q}$ by $\mathbf{r}_{\alpha}$. $d_{\alpha,j}^{\mathbf{k}}$ is the LCAO coefficient, which is obtained from the Schrödinger equation as follows:

$$\mathbf{h}(\mathbf{k})\mathbf{d}_j^{\mathbf{k}} = \lambda_j^{\mathbf{k}} \mathbf{S}(\mathbf{k})\mathbf{d}_j^{\mathbf{k}} \tag{2-1}$$

$$\mathbf{d}_j^{\mathbf{k}} = \left(d_{1,j}^{\mathbf{k}} \quad d_{2,j}^{\mathbf{k}} \quad \cdots \quad d_{\alpha,j}^{\mathbf{k}} \quad \cdots \quad d_{M,j}^{\mathbf{k}} \right)^T \tag{2-2}$$

$$\mathbf{h}(\mathbf{k}) = \sum_{\mathbf{Q}}^{K} \exp(i\mathbf{k}\cdot\mathbf{Q}) \mathbf{h}(\mathbf{Q}) \tag{2-3}$$

$$\mathbf{S}(\mathbf{k}) = \sum_{\mathbf{Q}}^{K} \exp(i\mathbf{k}\cdot\mathbf{Q}) \mathbf{S}(\mathbf{Q}) \tag{2-4}$$

$$\mathbf{d}_j^{\mathbf{k}*T} \mathbf{S}(\mathbf{k}) \mathbf{d}_{j'}^{\mathbf{k}} = \delta_{j,j'} . \tag{2-5}$$

Here, the Hamiltonian and the overlap matrices are given by $\left[\mathbf{h}(\mathbf{Q})\right]_{\alpha\beta} = \left\langle \chi_{\alpha}^{\mathbf{Q}_1} \middle| \hat{h} \middle| \chi_{\beta}^{\mathbf{Q}_2} \right\rangle$ and $\left[\mathbf{S}(\mathbf{Q})\right]_{\alpha\beta} = \left\langle \chi_{\alpha}^{\mathbf{Q}_1} \middle| \chi_{\beta}^{\mathbf{Q}_2} \right\rangle$, respectively. $\hat{h}$ is the one-electron Hamiltonian operator, and $\mathbf{Q} = \mathbf{Q}_2 - \mathbf{Q}_1$. The Hamiltonian matrix is composed of the following terms:

$$\mathbf{h}(\mathbf{Q}) = \mathbf{T}(\mathbf{Q}) + \mathbf{V}_{NA}(\mathbf{Q}) + \mathbf{V}_{Hartree}(\mathbf{Q}) + \mathbf{V}_{XC}(\mathbf{Q}) \tag{3}$$

Here, $\mathbf{T}(\mathbf{Q})$ represents the kinetic term, whose matrix element is obtained from $\left[\mathbf{T}(\mathbf{Q})\right]_{\alpha\beta} = \left\langle \chi_{\alpha}^{0} \middle| -(1/2)\nabla^2 \middle| \chi_{\beta}^{\mathbf{Q}} \right\rangle$. $\mathbf{V}_{NA}(\mathbf{Q})$ is the nuclear attraction term, which is obtained from $\left[\mathbf{V}_{NA}(\mathbf{Q})\right]_{\alpha\beta} = \left\langle \chi_{\alpha}^{0} \middle| \sum_A -\left(Z_A / |\mathbf{r} - \mathbf{R}_A|\right) \middle| \chi_{\beta}^{\mathbf{Q}} \right\rangle$, $\mathbf{V}_{Hartree}(\mathbf{Q})$ is the Hartree term, and $\mathbf{V}_{XC}(\mathbf{Q})$ is the exchange-correlation term. For example, the exchange-correlation term in the HF approximation is expressed using $r_{12} = |\mathbf{r}_1 - \mathbf{r}_2|$ as follows,

$$\left[\mathbf{V}^{Fock}(\mathbf{Q})\right]_{\alpha\beta} = -\sum_{\gamma}\sum_{\delta}\sum_{\mathbf{Q}_1,\mathbf{Q}_2} \mathbf{D}_{\gamma\delta}(\mathbf{Q}_1 - \mathbf{Q}_2) \iint \chi_{\alpha}^{0}(\mathbf{r}_1) \chi_{\gamma}^{\mathbf{Q}}(\mathbf{r}_1) \frac{1}{r_{12}} \chi_{\beta}^{\mathbf{Q}_1}(\mathbf{r}_2) \chi_{\delta}^{\mathbf{Q}_2}(\mathbf{r}_2) d\mathbf{r}_1 d\mathbf{r}_2 \tag{4}$$

Here the AO-basis density matrix $\mathbf{D}$ is obtained from the following equation.

$$D_{\alpha\beta}(\mathbf{Q}) = \frac{1}{K} \sum_{\mathbf{k}} \sum_{j} f_{FD}\left(E_F - \lambda_j^{\mathbf{k}}\right) d_{\alpha,j}^{\mathbf{k}*} d_{\beta,j}^{\mathbf{k}} \exp(i\mathbf{k}\cdot\mathbf{Q}) \tag{5}$$

Where $f_{FD}\left(E_F-\lambda_j^{\mathbf{k}}\right)$ and E_F are the Fermi–Dirac distribution function and the Fermi energy, respectively.

2.2 Gaussian and Fourier Transform (GFT) method

In the crystal orbital method, the calculation of the Hartree term is the most time-consuming part due to the long-range behavior of the Coulomb potential. The electron-electron repulsion integrals need to be summed up to achieve numerical convergence. In order to avoid the time-consuming integrations, we employ the Hartree (Coulomb) potential with the plane-wave description and the Fourier transform technique.(Shimazaki et al. 2009 a) In the method, we divided the nuclear attraction and Hartree terms into core and valence contributions as follows.

$$\mathbf{V}_{Hartree}\left(\mathbf{Q}\right)=\mathbf{V}_{Hartree}^{core}\left(\mathbf{Q}\right)+\mathbf{V}_{Hartree}^{valence}\left(\mathbf{Q}\right) \tag{6-1}$$

$$\mathbf{V}_{NA}\left(\mathbf{Q}\right)=\mathbf{V}_{NA}^{core}\left(\mathbf{Q}\right)+\mathbf{V}_{SR-NA}^{valence}\left(\mathbf{Q}\right)+\mathbf{V}_{LR-NA}^{valence}\left(\mathbf{Q}\right) \tag{6-2}$$

The above equation is obtained by simply dividing the terms into core and valence contributions, where $\mathbf{V}_{NA}^{core}\left(\mathbf{Q}\right)$ and $\mathbf{V}_{Hartree}^{core}\left(\mathbf{Q}\right)$ are the nuclear attraction and Hartree terms for the core contribution, respectively. $\mathbf{V}_{SR-NA}^{valence}\left(\mathbf{Q}\right)$ and $\mathbf{V}_{LR-NA}^{valence}\left(\mathbf{Q}\right)$ are the short-range (SR) and long-range (LR) nuclear attraction terms, respectively, for the valence contribution. $\mathbf{V}_{Hartree}^{valence}\left(\mathbf{Q}\right)$ is the Hartree term for the valence contribution. The electron-electron and electron-nuclear interactions of the core contribution are directly determined based on the conventional quantum chemical (direct lattice sum) calculations. However, this lattice sum calculations does not intensively consume CPU-time, because core electrons are strongly localized, and therefore its potential-tail rapidly decays to cancel the core nuclear charges. We will discuss the effective core potential (ECP) for core electrons in the next section. On the other hand, the contribution of valence electrons is considered by using the Poisson's equation and the Fourier transform. In order to divide the terms into core and valence contributions, we introduce the following core and valence electron densities.

$$\rho\left(\mathbf{r}\right)=\sum_{\alpha}\sum_{\beta}\sum_{\mathbf{Q}_1,\mathbf{Q}_2}\mathbf{D}_{\alpha\beta}\left(\mathbf{Q}_2-\mathbf{Q}_1\right)\chi_{\beta}^{\mathbf{Q}_2}\left(\mathbf{r}\right)\chi_{\alpha}^{\mathbf{Q}_1}\left(\mathbf{r}\right)\equiv\rho^{core}\left(\mathbf{r}\right)+\rho^{valence}\left(\mathbf{r}\right) \tag{7-1}$$

$$\rho^{valence}\left(\mathbf{r}\right)=\sum_{\alpha}^{valence}\sum_{\beta}^{valence}\sum_{\mathbf{Q}_1,\mathbf{Q}_3}\mathbf{D}_{\alpha\beta}\left(\mathbf{Q}_3\right)\chi_{\alpha}^{\mathbf{Q}_1}\left(\mathbf{r}\right)\chi_{\beta}^{\mathbf{Q}_1+\mathbf{Q}_3}\left(\mathbf{r}\right) \tag{7-2}$$

$$\rho^{core}\left(\mathbf{r}\right)=\rho\left(\mathbf{r}\right)-\rho^{valence}\left(\mathbf{r}\right) \tag{7-3}$$

Here, $\rho\left(\mathbf{r}\right)$ is the total electron density, and $\rho^{core}\left(\mathbf{r}\right)$ and $\rho^{valence}\left(\mathbf{r}\right)$ are the core and valence electron densities, respectively. The Hartree potential is divided into core and valence components on the basis of eq. (7) as follows:

$$\begin{aligned}V_{Hartree}\left(\mathbf{r}\right)&=\int\frac{\rho\left(\mathbf{r}'\right)}{\left|\mathbf{r}-\mathbf{r}'\right|}d\mathbf{r}'=\int\frac{\rho^{core}\left(\mathbf{r}'\right)}{\left|\mathbf{r}-\mathbf{r}'\right|}d\mathbf{r}'+\int\frac{\rho^{valence}\left(\mathbf{r}'\right)}{\left|\mathbf{r}-\mathbf{r}'\right|}d\mathbf{r}'\\&\equiv V_{Hartree}^{core}\left(\mathbf{r}\right)+V_{Hartree}^{valence}\left(\mathbf{r}\right)\end{aligned} \tag{8}$$

The "core" Hartree term in the GFT method is obtained from the "core" contribution of the density matrix as follows:

$$\begin{aligned}\left[\mathbf{V}_{Hartree}^{core}(\mathbf{Q})\right]_{\alpha\beta} &= \left\langle \chi_\alpha^0 \middle| V_{Hartree}^{core} \middle| \chi_\beta^{\mathbf{Q}} \right\rangle \\ &= \sum_\gamma^{core}\sum_\delta^{core}\sum_{\mathbf{Q}_1,\mathbf{Q}_2} D_{\gamma\delta}(\mathbf{Q}_1-\mathbf{Q}_2)\left\langle \chi_\alpha^0\chi_\gamma^{\mathbf{Q}_1} \middle| \chi_\beta^{\mathbf{Q}}\chi_\delta^{\mathbf{Q}_2} \right\rangle \\ &+\sum_\gamma^{core}\sum_\delta^{valence}\sum_{\mathbf{Q}_1,\mathbf{Q}_2} D_{\gamma\delta}(\mathbf{Q}_1-\mathbf{Q}_2)\left\langle \chi_\alpha^0\chi_\gamma^{\mathbf{Q}_1} \middle| \chi_\beta^{\mathbf{Q}}\chi_\delta^{\mathbf{Q}_2} \right\rangle \\ &+\sum_\gamma^{valence}\sum_\delta^{core}\sum_{\mathbf{Q}_1,\mathbf{Q}_2} D_{\gamma\delta}(\mathbf{Q}_1-\mathbf{Q}_2)\left\langle \chi_\alpha^0\chi_\gamma^{\mathbf{Q}_1} \middle| \chi_\beta^{\mathbf{Q}}\chi_\delta^{\mathbf{Q}_2} \right\rangle\end{aligned} \tag{9-1}$$

$$\left\langle \chi_\alpha^0\chi_\gamma^{\mathbf{Q}_1} \middle| \chi_\beta^{\mathbf{Q}}\chi_\delta^{\mathbf{Q}_2} \right\rangle = \iint \chi_\alpha^0(\mathbf{r}_1)\chi_\beta^{\mathbf{Q}}(\mathbf{r}_1)\frac{1}{r_{12}}\chi_\gamma^{\mathbf{Q}_1}(\mathbf{r}_2)\chi_\delta^{\mathbf{Q}_2}(\mathbf{r}_2)d\mathbf{r}_1 d\mathbf{r}_2 \tag{9-2}$$

The lattice sum over a small number of sites is required since the core electrons are strongly localized around the center of the nucleus and their electron charges are thus perfectly compensated by the core nuclear charges. On the other hand, the "valence" Hartree term in the GFT method can be taken into account through the following Poisson's equation, where we can employ Fourier transform technique to solve the equation.

$$\nabla^2 V_{Hartree}^{valence}(\mathbf{r}) = -4\pi\rho^{valence}(\mathbf{r}) \tag{10-1}$$

$$V_{Hartree}^{valence}(\mathbf{r}) = \frac{4\pi}{N_{FT}}\sum_{\mathbf{G}}\frac{\rho(\mathbf{G})}{G^2}\exp(i\mathbf{G}\cdot\mathbf{r}) \tag{10-2}$$

$$\rho(\mathbf{G}) \equiv \sum_{\mathbf{r}_g}\rho(\mathbf{r}_g)\exp(-i\mathbf{G}\cdot\mathbf{r}_g) \tag{10-3}$$

We can employ a fast Fourier transform (FFT) method, and $\mathbf{r}_g$ represents a grid point for the FFT calculations. Thus, the "valence" Hartree term is obtained as follows,

$$\left[\mathbf{V}_{Hartree}^{valence}(\mathbf{Q})\right]_{\alpha\beta} = \left\langle \chi_\alpha^0 \middle| V_{Hartree}^{valence} \middle| \chi_\beta^{\mathbf{Q}} \right\rangle = \frac{4\pi}{N_{FT}}\sum_{\substack{\mathbf{G}\\ G\neq 0}}\frac{\rho(\mathbf{G})}{G^2}\left\langle \chi_\alpha^0 \middle| \exp(i\mathbf{G}\cdot\mathbf{r}) \middle| \chi_\beta^{\mathbf{Q}} \right\rangle \tag{11}$$

In the above equation, we omit the term of $G=0$. The term will be discussed later.
The nuclear attraction potential is also divided into core and valence components:

$$V_{NA}(\mathbf{r}) = \sum_A \frac{Z_A}{|\mathbf{r}-\mathbf{R}_A|} = \sum_A \frac{Z_A^{core}}{|\mathbf{r}-\mathbf{R}_A|} + \sum_A \frac{Z_A^{valence}}{|\mathbf{r}-\mathbf{R}_A|} \equiv V_{NA}^{core}(\mathbf{r}) + V_{NA}^{valence}(\mathbf{r}) \tag{12}$$

Here, Z_A is the nuclear charge for atom number A. The "core" nuclear charge Z_A^{core} is defined as follows.

$$Z_A^{core} = \sum_{\alpha\in A}^{core}\sum_\beta^{core}\sum_{\mathbf{Q}} D_{a\beta}(\mathbf{Q})S_{\beta a}(\mathbf{Q}) + \sum_{\alpha\in A}^{core}\sum_\beta^{valence}\sum_{\mathbf{Q}} D_{a\beta}(\mathbf{Q})S_{\beta a}(\mathbf{Q}) + \sum_{\alpha\in A}^{valence}\sum_\beta^{core}\sum_{\mathbf{Q}} D_{a\beta}(\mathbf{Q})S_{\beta a}(\mathbf{Q}) \tag{13}$$

The remaining charge is assigned as the "valence" nuclear $Z_A^{valence}$ charge as follows.

$$Z_A^{valence} = Z_A - Z_A^{core} \tag{14}$$

The "core" nuclear attraction term is obtained as follows.

$$\left[\mathbf{V}_{NA}^{core}(\mathbf{Q})\right]_{\alpha\beta} = -\left\langle \chi_\alpha^{\mathbf{0}} \middle| V_{NA}^{core} \middle| \chi_\beta^{\mathbf{Q}} \right\rangle = -\left\langle \chi_\alpha^{\mathbf{0}} \middle| \sum_A \frac{Z_A^{core}}{|\mathbf{r}-\mathbf{R}_A|} \middle| \chi_\beta^{\mathbf{Q}} \right\rangle \tag{15}$$

Note that the "core" and "valence" nuclear charges are renewed in each self-consistent field (SCF) cycle. In the GFT method, the "valence" nuclear attraction potential is divided into short-range (SL) and long-range (LR) contributions, where $V_{NA}^{valence} = V_{SR-NA}^{valence} + V_{LR-NA}^{valence}$ by using the following error function (erf) and complementary error function (erfc).

$$\frac{1}{r} = \frac{erf(wr)}{r} + \frac{erfc(wr)}{r} \tag{16-1}$$

$$erf(wr) = \int_0^{wr} \exp(-t^2)\,dt \tag{16-2}$$

The short range (SR) "valence" nuclear attraction term is determined from the complementary error function (erfc) and the "valence" nuclear charges $Z_A^{valence}$ as follows,

$$\left[\mathbf{V}_{SR-NA}^{valence}(\mathbf{Q})\right]_{\alpha\beta} = -\left\langle \chi_\alpha^{\mathbf{0}} \middle| V_{SR-NA}^{valence} \middle| \chi_\beta^{\mathbf{Q}} \right\rangle = -\left\langle \chi_\alpha^{\mathbf{0}} \middle| \sum_A \frac{Z_A^{valence} erfc\left(\sqrt{\eta}\,|\mathbf{r}-\mathbf{R}_A|\right)}{|\mathbf{r}-\mathbf{R}_A|} \middle| \chi_\beta^{\mathbf{Q}} \right\rangle \tag{17}$$

The long range (LR) "valence" nuclear attraction term is obtained as follows,

$$\begin{aligned} \left[\mathbf{V}_{LR-NA}^{valence}(\mathbf{Q})\right]_{\alpha\beta} &= -\left\langle \chi_\alpha^{\mathbf{0}} \middle| \frac{Z_A^{valence} erf\left(\sqrt{\eta}\,|\mathbf{r}-\mathbf{R}_A|\right)}{|\mathbf{r}-\mathbf{R}_A|} \middle| \chi_\beta^{\mathbf{Q}} \right\rangle \\ &= -\frac{4\pi}{V_{cell}} \sum_A^{cell} \sum_{\substack{\mathbf{G} \\ (G\neq 0)}} \left(\frac{Z_Z^{valence}}{G^2}\right) \exp\left(-\frac{G^2}{4\eta}\right) \exp(-i\mathbf{G}\cdot\mathbf{R}_A) \int \chi_\alpha^{\mathbf{0}}(\mathbf{r})\,\chi_\beta^{\mathbf{Q}}(\mathbf{r}) \exp(i\mathbf{G}\cdot\mathbf{r})\,d\mathbf{r} \end{aligned} \tag{18}$$

In order to derive the above representation, we use the following equation.

$$\int \frac{erf\left(\sqrt{\eta}r\right)}{r} \exp(-i\mathbf{G}\cdot\mathbf{r})\,d\mathbf{r} = \frac{4\pi}{G^2} \exp\left(-\frac{4\eta}{G^2}\right) \tag{19}$$

Equation (18) does not include the term of $G = 0$. The term will be discussed with the corresponding term of the Hartree potential in the section 2.4.

2.3 Effective Core Potential (ECP) and total energy fourmula

If the effective core potential (ECP) is employed together with the GFT method, the core electron density, $\rho^{core}(\mathbf{r})$, and nuclear charges, Z_A^{core}, become zero, and the ECP term of

$\mathbf{V}_{ECP}$ is used for the Fock matrix instead of core contributions of the nuclear attraction and Hartree terms as follows,

$$\begin{aligned}\mathbf{h}(\mathbf{Q}) &= \mathbf{T}(\mathbf{Q}) + \mathbf{V}_{ECP}(\mathbf{Q}) + \mathbf{V}_{SR-NA}(\mathbf{Q}) \\ &+ \mathbf{V}_{LR-NA}(\mathbf{Q}) + \mathbf{V}_{Hartree}(\mathbf{Q}) + \mathbf{V}_{XC}(\mathbf{Q})\end{aligned} \tag{20}$$

The total energy per unit cell in this scheme is obtained as follows,

$$\begin{aligned}E_{total} &= \sum_{\alpha,\beta}\sum_{\mathbf{Q}} D_{\alpha\beta}(\mathbf{Q})\left\{\left[\mathbf{T}(\mathbf{Q})\right]_{\alpha\beta} + \left[\mathbf{V}_{ECP}(\mathbf{Q})\right]_{\alpha\beta} + \left[\mathbf{V}_{SR-NA}(\mathbf{Q})\right]_{\alpha\beta}\right\} \\ &+ E_{XC} + \sum_{\substack{\mathbf{G} \\ (G\neq 0)}} \frac{1}{2}\frac{4\pi V_{cell}}{N_{FT}^2}\frac{\left|\rho(\mathbf{G})\right|^2}{G^2} + \frac{\pi}{\eta V_{cell}}\left(\sum_{A}^{cell} Z_A\right)\sum_{\mathbf{Q}}\sum_{\alpha\beta} D_{\alpha\beta}(\mathbf{Q}) S_{\beta\alpha}(\mathbf{Q}) \\ &- \frac{4\pi}{N_{FT}}\sum_{A}^{cell}\sum_{\substack{\mathbf{G} \\ (G\neq 0)}} \frac{Z_A\rho(\mathbf{G})}{G^2}\exp\left(-\frac{G^2}{4\eta}\right)\exp(i\mathbf{G}\cdot\mathbf{R}_A) + \frac{1}{2}\sum_{\mathbf{Q}}\sum_{\substack{A,B}}^{cell}{}_{(\mathbf{R}_A-\mathbf{R}_B-\mathbf{Q}\neq\mathbf{0})} \frac{Z_A Z_B\, erfc\left(\sqrt{\eta}\left|\mathbf{R}_A-\mathbf{R}_B-\mathbf{Q}\right|\right)}{\left|\mathbf{R}_A-\mathbf{R}_B-\mathbf{Q}\right|} \\ &+ \frac{1}{2}\frac{4\pi}{V_{cell}}\sum_{\substack{\mathbf{G} \\ (G\neq 0)}}\sum_{A,B}^{cell} Z_A Z_B \frac{1}{G^2}\exp\left(-\frac{G^2}{4\eta}\right)\exp\left(i\mathbf{G}\cdot(\mathbf{R}_B-\mathbf{R}_A)\right) \\ &- \left(\sum_A Z_A^2\right)\sqrt{\frac{\eta}{\pi}} - \frac{1}{2}\left[\sum_A^{cell} Z_A\right]^2\frac{\pi}{\eta V_{cell}}\end{aligned} \tag{21}$$

Here, $\mathbf{G}$ is the reciprocal lattice vector. E_{XC} is the exchange-correlation energy of the unit cell, which is written as $E_{XC} = 0.5\sum_{\mathbf{Q}} Tr\left[\mathbf{D}(\mathbf{Q})\mathbf{V}_X^{Fock}(\mathbf{Q})\right]$ in the Hartree-Fock approximation. N_{FT} is the number of grids for the Fourier transform. $\rho(\mathbf{G}) = \sum_{\mathbf{r}_g}\rho(\mathbf{r}_g)\exp(-i\mathbf{G}\cdot\mathbf{r}_g)$, where $\mathbf{r}_g$ is the grid point for FFT calculations. Last four terms of the total energy come from the Ewald-type representation for the nuclear-nuclear repulsion energy.

2.4 Constant term

In this section, we discuss the terms of $G=0$, which appears in the nuclear attraction and Hartree terms, and the nuclear-nuclear repulsion. The total energy formula of eq. (21) includes the constant terms, which are derived from considerations of $G=0$. The Fourier coefficient of the electron density behaves in the limit of $G=0$ as follows,

$$\begin{aligned}&\lim_{G\to 0}\rho(G) = \lim_{G\to 0}\sum_{\mathbf{r}_g}\rho(\mathbf{r}_g)\exp(-i\mathbf{G}\cdot\mathbf{r}_g) \\ &\simeq \lim_{G\to 0}\left[\sum_{\mathbf{r}_g}\rho(\mathbf{r}_g)\left(1 - iGr_g\cos\theta + \frac{1}{2}G^2 r_g^2\cos^2\theta\right)\right] \\ &\approx \sum_{\mathbf{r}_g}\rho(\mathbf{r}_g) + \beta G^2 = N_{FT}\bar{\rho} + \beta G^2\end{aligned} \tag{22}$$

Here, we use $\lim_{G\to 0}\sum_{\mathbf{r}_g}\rho(\mathbf{r}_g)\left(-iGr_g\cos\theta\right)=0$ and $\bar{\rho}=\left(1/N_{FT}\right)\sum_{\mathbf{r}_g}\rho(\mathbf{r}_g)$. β is a constant, however it disappears in the final form of the total energy, as shown bellow. On the other hand, the Hartree energy per unit cell is determined from the following equation:

$$\begin{aligned} E_{Hartree} &= \frac{1}{2}\int_{V_{cell}} V_{ele}(\mathbf{r})\rho(\mathbf{r})d\mathbf{r} \\ &= \int_{V_{cell}} \frac{4\pi}{N_{FT}}\sum_{\mathbf{G}}\frac{\rho(\mathbf{G})}{G^2}\exp(i\mathbf{G}\cdot\mathbf{r})\frac{1}{N_{FT}}\sum_{\mathbf{G}'}\rho(\mathbf{G}')\exp(i\mathbf{G}'\cdot\mathbf{r})d\mathbf{r} \\ &= \frac{4\pi}{N_{FT}^2}\sum_{\mathbf{G},\mathbf{G}'}\frac{1}{G^2}\rho(\mathbf{G})\rho(\mathbf{G}')V_{cell}\delta_{\mathbf{G}',-\mathbf{G}} = \frac{4\pi}{N_{FT}^2}V_{cell}\sum_{\mathbf{G}}\frac{\left|\rho(\mathbf{G})\right|^2}{G^2} \end{aligned} \tag{23}$$

Here, we use $\left(1/V_{cell}\right)\int_{V_{cell}}\exp\left(i\left(\mathbf{G}-\mathbf{G}'\right)\cdot\mathbf{r}\right)d\mathbf{r}=\delta_{\mathbf{G},\mathbf{G}'}$ and $\rho^*(\mathbf{G})=\rho(-\mathbf{G})$. If we consider the limit of $G=0$, the Hartree energy can be described as follows,

$$\begin{aligned} E_{Hartree} &= \frac{1}{2}\frac{4\pi}{N_{FT}^2}V_{cell}\sum_{\mathbf{G},(G\neq 0)}\frac{\left|\rho(\mathbf{G})\right|^2}{G^2}+\lim_{G\to 0}\frac{1}{2}\frac{4\pi}{N_{FT}^2}V_{cell}\frac{\left|\rho(\mathbf{G})\right|^2}{G^2} \\ &\approx \sum_{\mathbf{G},(G\neq 0)}\frac{1}{2}\frac{4\pi}{N_{FT}^2}V_{cell}\frac{\left|\rho(\mathbf{G})\right|^2}{G^2}+\lim_{G\to 0}\frac{1}{2}\frac{4\pi}{N_{FT}^2}V_{cell}\frac{\left(N_{FT}\bar{\rho}+\beta G^2\right)\left(N_{FT}\bar{\rho}+\beta G^2\right)}{G^2} \\ &\approx \sum_{\mathbf{G},(G\neq 0)}\frac{1}{2}\frac{4\pi V_{cell}}{N_{FT}^2}\frac{\left|\rho(\mathbf{G})\right|^2}{G^2}+\lim_{G\to 0}\frac{1}{2}4\pi V_{cell}\bar{\rho}^2\frac{1}{G^2}+\frac{4\pi}{N_{FT}}V_{cell}\beta\bar{\rho} \end{aligned} \tag{24}$$

Next, we discuss the long-range nuclear attraction energy.

$$\begin{aligned} E_{LR-NA} &= -\int_{V_{cell}} V_{LR-NA}(\mathbf{r})\rho(\mathbf{r})d\mathbf{r} \\ &= -\int_{V_{cell}}\frac{4\pi}{V_{cell}}\sum_{\mathbf{G}}\sum_{A}^{cell}Z_A\frac{1}{G^2}\exp\left(-\frac{G^2}{4\eta}\right)\exp\left(i\mathbf{G}\cdot\left(\mathbf{r}-\mathbf{R}_A\right)\right)\frac{1}{N_{FT}}\sum_{\mathbf{G}'}\rho(\mathbf{G}')\exp(i\mathbf{G}'\cdot\mathbf{r})d\mathbf{r} \\ &= -\frac{4\pi}{N_{FT}}\sum_{A}^{cell}\sum_{\mathbf{G}}Z_A\frac{1}{G^2}\exp\left(-\frac{G^2}{4\eta}\right)\exp(i\mathbf{G}\cdot\mathbf{R}_A)\rho(\mathbf{G}) \end{aligned} \tag{25}$$

Then, the following asymptotic equation is obtained from the above term in the $G\to 0$ case.

$$\begin{aligned} -\lim_{G\to 0}\frac{4\pi}{N_{FT}}\sum_{A}^{cell}\frac{Z_A\rho(\mathbf{G})}{G^2}\exp\left(-\frac{G^2}{4\eta}\right)\exp(i\mathbf{G}\cdot\mathbf{R}_A) &\approx -\lim_{G\to 0}\frac{4\pi}{N_{FT}}\sum_{A}^{cell}\frac{Z_A\left(1-\frac{G^2}{4\eta}\right)\left(N_{FT}\bar{\rho}+\beta G^2\right)}{G^2} \\ &\approx -\lim_{G\to 0}4\pi\left(\sum_{A}^{cell}Z_A\right)\bar{\rho}\frac{1}{G^2}-\frac{4\pi}{N_{FT}}\left(\sum_{A}^{cell}Z_A\right)\beta+4\pi\left(\sum_{A}^{cell}Z_A\right)\bar{\rho}\frac{1}{4\eta} \\ &= -\lim_{G\to 0}4\pi V_{cell}\bar{\rho}^2\frac{1}{G^2}-\frac{4\pi}{N_{FT}}V_{cell}\beta\bar{\rho}+\frac{\pi}{\eta V_{cell}}\left(\sum_{A}^{cell}Z_A\right)\sum_{\mathbf{Q}}\sum_{\alpha\beta}\mathbf{D}_{\alpha\beta}^{\mathbf{Q}}\mathbf{S}_{\alpha\beta}^{\mathbf{Q}} \end{aligned} \tag{26}$$

Here, $\sum_A^{cell} Z_A = V_{cell}\bar{\rho}$ and $\sum_A Z_A = \sum_{\mathbf{r}_g} \rho(\mathbf{r}_g)$. The second term of eq. (26), which includes β, is cancelled out by the corresponding constant term of the Hartree energy of eq. (24).
The asymptotic description for nucleus-nucleus repulsion term is obtained from the Ewald-type long range interaction as follows,

$$\begin{aligned}
&\lim_{G\to 0}\frac{1}{2}\frac{4\pi}{V_{cell}}\sum_{A,B}^{cell} Z_A Z_B \frac{1}{G^2}\exp\left(-\frac{G^2}{4\eta}\right)\exp\left(i\mathbf{G}\cdot(\mathbf{R}_B-\mathbf{R}_A)\right)\\
&\simeq \lim_{G\to 0}\frac{1}{2}\frac{4\pi}{V_{cell}}\sum_{A,B}^{cell} Z_A Z_B \frac{1}{G^2}\left(1-\frac{G^2}{4\eta}\right)\\
&= \lim_{G\to 0}\frac{1}{2}4\pi V_{cell}\bar{\rho}^2\frac{1}{G^2} - \frac{1}{2}\left[\sum_A^{cell} Z_A\right]^2\frac{\pi}{\eta V_{cell}}
\end{aligned} \tag{27}$$

The first term of eq. (27) is cancelled by the corresponding terms of eqs (24) and (26). The compensation of the self-interaction of the long-range nucleus-nucleus interaction also brings in the constant term, and the term can be obtained from $A=B$ in the long-range nucleus-nucleus interaction as follows,

$$\begin{aligned}
&\frac{1}{2}\frac{4\pi}{V_{cell}}\sum_{\mathbf{G}}\sum_A^{cell} Z_A^2\frac{1}{G^2}\exp\left(-\frac{G^2}{4\eta}\right)\exp(i\mathbf{G}\cdot\mathbf{0})\\
&= \frac{1}{2}\sum_A^{cell} Z_A^2 \lim_{r\to\infty}\frac{erf\left(\sqrt{\eta}r\right)}{r} = \sum_A^{cell} Z_A^2\sqrt{\frac{\eta}{\pi}}
\end{aligned} \tag{28}$$

Here, we use $\lim_{r\to 0} erf\left(\sqrt{\eta}r\right)/r \approx 2\sqrt{\eta/\pi}$.

2.5 Recursion relation

In order to obtain the integrations in eqs (11) and (18), we can use the following recursion relation.

$$\begin{aligned}
&\left\langle \mathbf{a}+\mathbf{1}_\xi \middle| \exp(i\mathbf{G}\cdot\mathbf{r}) \middle| \mathbf{b}\right\rangle = \left(P_\xi - R_\xi^A + \frac{iG_\xi}{2p}\right)\left\langle \mathbf{a}\middle|\exp(i\mathbf{G}\cdot\mathbf{r})\middle|\mathbf{b}\right\rangle\\
&+\frac{1}{2p}N_\xi(\mathbf{a})\left\langle \mathbf{a}-\mathbf{1}_\xi\middle|\exp(i\mathbf{G}\cdot\mathbf{r})\middle|\mathbf{b}\right\rangle + \frac{1}{2p}N_\xi(\mathbf{b})\left\langle \mathbf{a}\middle|\exp(i\mathbf{G}\cdot\mathbf{r})\middle|\mathbf{b}-\mathbf{1}_\xi\right\rangle
\end{aligned} \tag{29-1}$$

$$\left\langle \mathbf{0}\middle|\exp(i\mathbf{G}\cdot\mathbf{r})\middle|\mathbf{0}\right\rangle = \exp\left(-\mu\left|\mathbf{R}_A-\mathbf{R}_B\right|^2\right)\left(\frac{\pi}{p}\right)^{\frac{3}{2}}\exp\left(-\frac{G^2}{4p}\right)\exp(i\mathbf{G}\cdot\mathbf{P}) \tag{29-2}$$

$$\left|\mathbf{a}\right\rangle = \left(x-R_x^A\right)^{a_x}\left(y-R_y^A\right)^{a_y}\left(z-R_z^A\right)^{a_z}\exp\left(-g_a\left|\mathbf{r}-\mathbf{R}_A\right|^2\right) \tag{29-3}$$

Here, $p=g_a+g_b$, $\mu = g_a g_b/(g_a+g_b)$, $\mathbf{a}=(a_x \quad a_y \quad a_z)$, $N_\xi(\mathbf{a})=a_\xi$, and $\mathbf{1}_\xi=(\delta_{x\xi} \quad \delta_{y\xi} \quad \delta_{z\xi})$ using Kronecker's delta. $\mathbf{P}=(g_a\mathbf{R}_A+g_b\mathbf{R}_b)/(g_a+g_b)$. ξ represents one of x, y, or z. The

recursion relation is an expansion of the Obara and Saika (OS) technique for atomic orbital (AO) integrals.(Obara et al. 1986)

3. Screened Hartree-Fock exchange potential

3.1 Dielectric function and screened exchange potential

The screening effect caused by electron correlations is an important factor in determining the electronic structure of solid-state materials. The Fock exchange term can be represented as a bare interaction between electron and exchange hole in the Hartree–Fock approximation.(Parr et al. 1994) The electron correlation effect screens the interaction. In this section, we discuss the screening effect for bulk materials, especially semiconductors.

The screening effect is closely related to the electric part of the dielectric function. The Thomas–Fermi model is a well-known dielectric model function for free electron gas.(Yu et al. 2005; Ziman 1979)

$$\varepsilon^{TF}\left(\mathbf{k}\right)=1+\left[\left(\frac{k^2}{k_{TF}^2}\right)\right]^{-1} \tag{30}$$

Here, k_{TF} is the Thomas–Fermi wave number. Although the Thomas–Fermi model is applicable for metallic system, it is not suitable to semiconductors because it diverges when $k=0$. The dielectric constant of semiconductors must take a finite value at $k=0$. Therefore, a number of different dielectric function models for semiconductors have been proposed for semiconductors,(Levine et al. 1982; Penn 1962) and Bechstedt et al. proposed the following model to reproduce the property of semiconductors.(Bechstedt et al. 1992; Cappellini et al. 1993)

$$\varepsilon^{Bechstedt}\left(\mathbf{k}\right)=1+\left[\left(\varepsilon_s-1\right)^{-1}+\alpha\left(\frac{k^2}{k_{TF}^2}\right)+\frac{k^4}{4k_F^2k_{TF}^2/3}\right]^{-1} \tag{31}$$

Here, k_F is the Fermi wave number whose value depends on the average electron density. ε_s is the electric part of the dielectric constant. The value of coefficient α is determined in such way that it fits to the random phase approximation (RPA) calculation, and Bechstedt et al. reported that the values of α do not display a strong dependence on the material type. In this paper, we employ $\alpha=1.563$ according to their suggestion. The most important point is that the Bechstedt's model does not diverge at $k=0$; $\varepsilon^{Bechstedt}\left(k=0\right)=\varepsilon_s$. In this paper, we simplify Bechstedt's model, and employ the following dielectric function model.

$$\varepsilon\left(\mathbf{k}\right)=1+\left[\left(\varepsilon_s-1\right)^{-1}+\alpha\left(\frac{k^2}{k_{TF}^2}\right)\right]^{-1} \tag{32}$$

The following equation is obtained from the above equation through the inversion.

$$\frac{1}{\varepsilon\left(\mathbf{k}\right)}=\left(1-\frac{1}{\varepsilon_s}\right)\frac{k^2}{k^2+\tilde{k}_{TF}^2}+\frac{1}{\varepsilon_s} \tag{33-1}$$

$$\tilde{k}_{TF}^2 = \frac{k_{TF}^2}{\alpha}\left(\frac{1}{\varepsilon_s - 1} + 1\right) \tag{33-2}$$

Then, we obtain the following screened potential from these equations and the Fourier transform.

$$V(\mathbf{r}) = \frac{1}{(2\pi)^3}\int \frac{4\pi}{k^2 \varepsilon(\mathbf{k})}\exp(i\mathbf{k}\cdot\mathbf{r})\,d\mathbf{k} = \left(1 - \frac{1}{\varepsilon_s}\right)\frac{\exp\left(-\tilde{k}_{TF} r\right)}{r} + \frac{1}{\varepsilon_s}\frac{1}{r} \tag{34}$$

The first term in the above equation represents the short range screened potential. However, since the screening effect is not complete in the semiconductors, the partial bare interaction appears in the second term. Conversely, for metallic systems, i.e., $\varepsilon_s \to \infty$, complete screening is achieved, and the second term disappears.

The Yukawa type potential, $\exp(-q_Y r)/r$, is difficult to handle with Gaussian basis sets, and therefore we employ $erfc(wr)/r$ instead of the Yukawa potential because the both functions behaves similarly if the relation $q_Y = 3w/2$ holds true.(Shimazaki et al. 2008) The use of a complementary error function provides a highly efficient algorithm for calculating Gaussian-based atomic orbital integrals. Thus, we obtain the following approximation.

$$V(\mathbf{r}) \approx \left(1 - \frac{1}{\varepsilon_s}\right)\frac{erfc\left(2\tilde{k}_{TF} r/3\right)}{r} + \frac{1}{\varepsilon_s}\frac{1}{r} \tag{35}$$

Based on the above discussions, we employ the following screened Fock exchange in this paper.

$$\begin{aligned}\left[\mathbf{V}_X^{screened}(w,\varepsilon_s)\right]_{\alpha\beta} &= -\sum_{\gamma,\delta} D_{\gamma\delta}\iint \chi_\alpha(\mathbf{r}_1)\chi_\gamma(\mathbf{r}_1) \\ &\times\left[\left(1 - \frac{1}{\varepsilon_s}\right)\frac{erfc(wr_{12})}{r_{12}} + \frac{1}{\varepsilon_s}\frac{1}{r_{12}}\right]\chi_\beta(\mathbf{r}_2)\chi_\delta(\mathbf{r}_2)\,d\mathbf{r}_1 d\mathbf{r}_2 \\ &\equiv \left(1 - \frac{1}{\varepsilon_s}\right)\left[\mathbf{V}_{SR-X}^{erfc}(w)\right]_{\alpha\beta} + \frac{1}{\varepsilon_s}\left[\mathbf{V}_X^{Fock}\right]_{\alpha\beta}\end{aligned} \tag{36}$$

Here, $w = 2\tilde{k}_{TF}/3$. The screened Fock exchange includes parameters such as $\tilde{k}_{TF}$ and ε_s, which strongly depend on the material. When $\varepsilon_s = 1$, eq. (36) reduces to the ordinary Fock exchange; $\mathbf{V}_X^{screened}(\tilde{k}_{TF}, 1) = \mathbf{V}_X^{HF}$.

3.2 Local potential approximation

The semiconductors discussed in this paper have a large Thomas-Fermi wave vector; thus, the screening length becomes small and the first term of eq. (36) mainly takes into account short-range interactions and small non-local contributions. This potentially allows the first term to be approximated by a local potential and to neglect its non-local contribution. In this paper, we examine the LDA functional as a replacement for the first term of eq. (36). Although the LDA functional is not the same as the local component of first term of eq. (36), this replacement can expand the scope of eq. (36), because electron correlations other than

the screening effect can be taken into account through the LDA functional. We should note that Bylander et al. employed a similar strategy.(Bylander et al. 1990) In this paper, we examine the following potentials:

$$\mathbf{V}^{screened}\left(\varepsilon_s\right)=\left(1-\frac{1}{\varepsilon_s}\right)\mathbf{V}^{Slater}+\frac{1}{\varepsilon_s}\mathbf{V}^{Fock} \tag{37}$$

$$\mathbf{V}^{screened}\left(\varepsilon_s\right)=\left(1-\frac{1}{\varepsilon_s}\right)\mathbf{V}^{Slater}+\frac{1}{\varepsilon_s}\mathbf{V}^{Fock}+\mathbf{V}^{VWN} \tag{38}$$

Here, $\mathbf{V}^{Slater}$ is the Slater exchange term, and $\mathbf{V}^{VWN}$ is the Vosko-Wilk-Nusair (VWN) correlation term. The above potentials appear to be types of hybrid-DFT functional. The relation between the screened HF exchange potential and the hybrid-DFT functional is discussed later. Equations (37) and (38) have a system-dependent HF exchange fraction, which is unusual for the ordinal hybrid-DFT method. In metal systems, that is, $\varepsilon_s \to \infty$, the above potential reduces to the ordinal LDA functional. It is worth noting that eqs. (37) and (38) depend on only ε_s, although eq. (36) depends on two parameters, namely, $\tilde{k}_{TF}$ and ε_s.

3.3 Self consistent scheme for dielectric constant

In eqs (36), (37), and (38), the fraction of the Fock exchange term is proportional to the inverse of the dielectric constant. Consequently, in order to use these equations, we must know the value of the dielectric constant for the target semiconductor. Although an experimentally obtained value is a possible candidate, here we discuss a self-consistent scheme for theoretically considering the dielectric constant. In this scheme, the static dielectric constant is assumed to be obtained from the following equations: (Ziman 1979)

$$\varepsilon_s = 1+\left(\omega_p \Big/ \overline{E}_{gap}\right)^2 \tag{39-1}$$

$$\overline{E}_{gap}=\frac{1}{K}\sum_{\mathbf{k}}^{K}\left(\lambda_{LUMO}^{\mathbf{k}}-\lambda_{HOMO}^{\mathbf{k}}\right) \tag{39-2}$$

Here, $\lambda_{HOMO}^{\mathbf{k}}$ and $\lambda_{LUMO}^{\mathbf{k}}$ are the HOMO and LUMO energies, respectively, at wave vector $\mathbf{k}$. $\overline{E}_{gap}$ is the average energy gap, and ω_p is the plasma frequency, the value of which is obtained from $\omega_p=\sqrt{4\pi n_e^{valence}}$. Equation (39-1) depends on the averaged energy gap because the dielectric constant reflects overall responses of k-space. The equation is combined with equations (36), (37), or (38) in the self-consistent-field (SCF) loop, and ε_s and $\overline{E}_{gap}$ are calculated and renewed in each SCF step. Here, the fraction of the HF exchange term, which is proportional to ε_s^{-1}, is not constant throughout the SCF cycle. We obtain the self-consistent dielectric constant and the energy band structure after the iterative procedure. Notably, this self-consistent scheme does not refer to any experimental results.

4. Application for GFT method and screened HF exchange potential

4.1 Diamond, silicon, AlP, AlAs, GaP, and GaAs

In this section, we present the energy band structures of the following semiconductors: diamond (C), silicon (Si), AlP, AlAs, GaP, and GaAs. We discuss the electronic structures of these semiconductors on the basis of the HF method, the local density approximation (LDA), and the hybrid-DFT method. The Slater–Vosko–Wilk–Nusair (SVWN) functional (Slater 1974; Vosko et al. 1980) and the B3LYP functional,(Becke 1993 b) the latter of which includes 80% of the Slater local density functional $\mathbf{V}^{Slater}$, 72% of the Becke88 (B88)-type gradient correction $\Delta\mathbf{V}^{B88}$ (Becke 1988) , and 20% of the HF exchange term, are employed for the LDA and the hybrid-DFT calculations, respectively. The B3LYP functional is shown below:(Becke 1993 b)

$$\mathbf{V}_{XC}^{B3LYP} = 0.8\mathbf{V}^{Slater} + 0.72\Delta\mathbf{V}^{B88} + 0.2\mathbf{V}^{Fock} + \mathbf{V}_{C}^{B3LYP} \tag{40-1}$$

$$\mathbf{V}_{C}^{B3LYP} = 0.19\mathbf{V}_{C}^{VWN} + 0.81\mathbf{V}_{C}^{LYP} \tag{40-2}$$

Here, $\mathbf{V}_{C}^{LYP}$ is the Lee–Yang–Parr correlation functional.(Lee et al. 1988) We used the 6-21G* basis set, which was proposed by Catti et al.(Catti et al. 1993), for diamond calculations. On the other hand, we employ the effective core potential proposed by Stevens et al. for silicon, AlP, AlAs, GaP, and GaAs.(Stevens et al. 1984; Stevens et al. 1992) The exponents and contraction coefficients listed in our previous paper are employed for the atomic orbitals for Si, Al, P, As, and Ga.(Shimazaki et al. 2010) We employ $24\times24\times24$ k-points for the Fourier transform technique, and $25\times25\times25$ mesh grid points are used, to calculate the valence electron contribution of the Hartree term. In addition to these, we employ the truncation condition of third neighboring cells. It should be noted that the truncation affect only the HF exchange and "core" Hartree (Coulomb) terms. In this section, we also present calculation results obtained from the screening HF exchange potential.

	C	Si	AlP	AlAs	GaP	GaAs
Lattice constant	6.74	10.26	10.30	10.70	10.30	10.68
V_{cell}	76.76	207.11	273.10	305.90	273.10	304.29
r_s	1.32	2.01	2.01	2.09	2.01	2.09
k_{Fermi}	1.46	0.96	0.95	0.92	0.95	0.92
k_{TF}	1.36	1.10	1.10	1.08	1.10	1.08
ε_s	5.65	12.1	7.54	8.16	10.75	12.9
$\tilde{k}_{TF}$	1.2	0.92	0.95	0.92	0.93	0.90
ε_s^{-1}	0.18	0.083	0.13	0.12	0.093	0.078

Table 1. Parameters for semiconductors in atomic unit [a.u.]

Table 1 presents the lattice constants and the dielectric constants of those semiconductors; the lattice constant, the volume of the unit cell V_{cell}, and the screening parameters are given in atomic units (a.u.). Here, the eight valence electrons in the unit cell are considered for

calculating the screening parameters. These parameters are used in the screened HF exchange potential, for example ε_s in Table 1 is used for eqs (36), (37), and (38). On the other hand, calculation results based on the self-consistent procedure are presented in Section 3.2.
Table 2 presents the direct and indirect bandgaps calculated by the SVWN, HF, and B3LYP methods for semiconductors, here we also show experimental bandgap values (Yu et al. 2005). The direct bandgap of GaAs is the same as the minimum energy difference. The SVWN functional underestimates the bandgaps in comparison with the experimental ones. The kind of underestimation is a well-known problem of LDA. On the other hand, the HF method overestimates the bandgap properties, and the B3LYP method yields better calculation results. However, the calculation results of B3LYP are more complex than the LDA and HF; for example, the B3LYP functional gives calculation results that are close to the experimental bandgap in diamond case, but the same functional overestimates the bandgaps for AlAs, AlP, and GaP. The B3LYP functional yields the indirect bandgap of 3.3 eV for AlAs, whereas the experimental property is 2.2 eV. While the B3LYP functional gives 3.6 eV for the indirect bandgap of AlP, the experimental one is 2.5 eV. In the case of GaP, the B3LYP and experimental bandgaps are 3.3 eV and 2.4 eV, respectively. The B3LYP functional can reproduce the experimental band structure of diamond well, however the results are poorer for other semiconductors such as AlAs, AlP, and GaP.

		HF [ev]	SVWN [eV]	B3LYP [eV]	Exp.[eV]
C	Direct	14.6	5.9	7.4	7.3
	Indirect	12.6	4.2	6.0	5.48
Si	Direct	8.0	2.0	3.3	3.48
	Indirect	6.1	0.50	1.8	1.11
AlP	Direct	11.4	4.0	5.6	3.6
	Indirect	8.5	2.0	3.6	2.5
AlAs	Direct	9.6	2.7	4.0	3.13
	Indirect	7.8	1.7	3.3	2.23
GaP	Direct	9.1	2.2	3.5	2.89
	Indirect	8.0	1.9	3.3	2.39
GaAs	Direct	6.8	0.86	1.91	1.52

Table 2. Theoretical and experimental bandgaps of semiconductors [eV]

Next, we discuss the screened HF exchange potential discussed in Section 3. The direct and indirect bandgaps calculated by the screened HF exchange potential are presented in Table 3. The overall calculation results are better than those from the SVWN, HF, and B3LYP methods. Equation (36) tends to underestimate the indirect bandgap, however eqs (37) and (38), which use the Slater functional instead of $\mathbf{V}_{SR-X}^{erfc}(w)$, show good agreement with the experimental results. The underestimation obtained from eq. (36) may cause that the equation takes into account only the screening effect. On the other hand, the VWN correlation functional of eq. (38) slightly improves the calculation results.
However, it should be noted that there is a lager gap between the experimental direct bandgap of AlP and our calculation result. The experimental value determined by photoluminescence spectroscopy is 3.62 eV (Monemar 1973), and our calculation result of eq. (38) is 4.9 eV. Zhu et al. noted that the experimentally obtained spectrum was broad and poorly defined due to a high concentration of defects in the AlP sample.(Zhu et al. 1991)

They also contended that the transition from Γ_{15v} to X_{3c} was assigned in error. They calculated 4.38 eV as the direct bandgap by the GW method, which is closer to our calculation result.

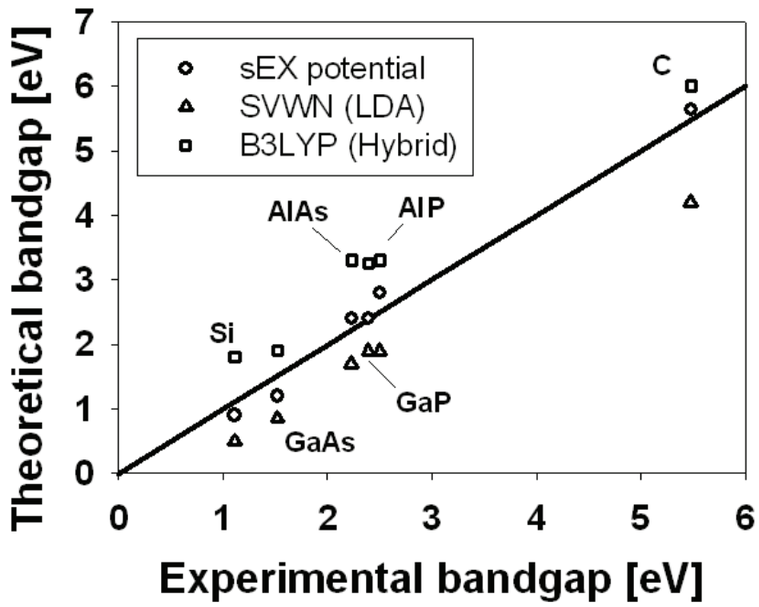

Fig. 1. Experimental and theoretical bandgap properties. Circles indicate calculation results based on screened HF exchange method (sEX) of eq. (38) with experimental dielectric constant, and triangles and squares denote SVWN and B3LYP results, respectively

		Eq. (36) [eV]	Eq. (37) [eV]	Eq. (38) [eV]
C	Direct	7.1	6.9	7.0
	Indirect	5.0	5.5	5.6
Si	Direct	2.4	2.4	2.5
	Indirect	0.44	0.77	0.90
AlP	Direct	5.1	4.9	5.0
	Indirect	2.1	2.6	2.8
AlAs	Direct	3.6	3.4	3.4
	Indirect	1.6	2.2	2.4
GaP	Direct	2.8	2.6	2.7
	Indirect	1.9	2.2	2.4
GaAs	Direct	1.4	1.2	1.2

Table 3. Bandgaps obtained from screened HF exchange potential with experimental ε_s

The theoretical bandgaps of diamond, silicon, AlP, AlAs, GaP, and GaAs, which are obtained from SVWN, B3LYP, and eq. (38), are shown with the experimental bandgaps in Figure 1. From the figure, we can easily confirm that the LDA (SVWN) functional underestimates the experimental bandgap. On the other hand, the B3LYP method reproduces the experimental results for diamond well, but overestimates AlP, AlAs, and GaP. The screened HF exchange potential shows good agreements with experiment (Yu et

al. 2005). The energy band structures of diamond, silicon, AlP, AlAs, GaP, and GaAs, which are obtained from eq. (38), are presented in Figure 2.

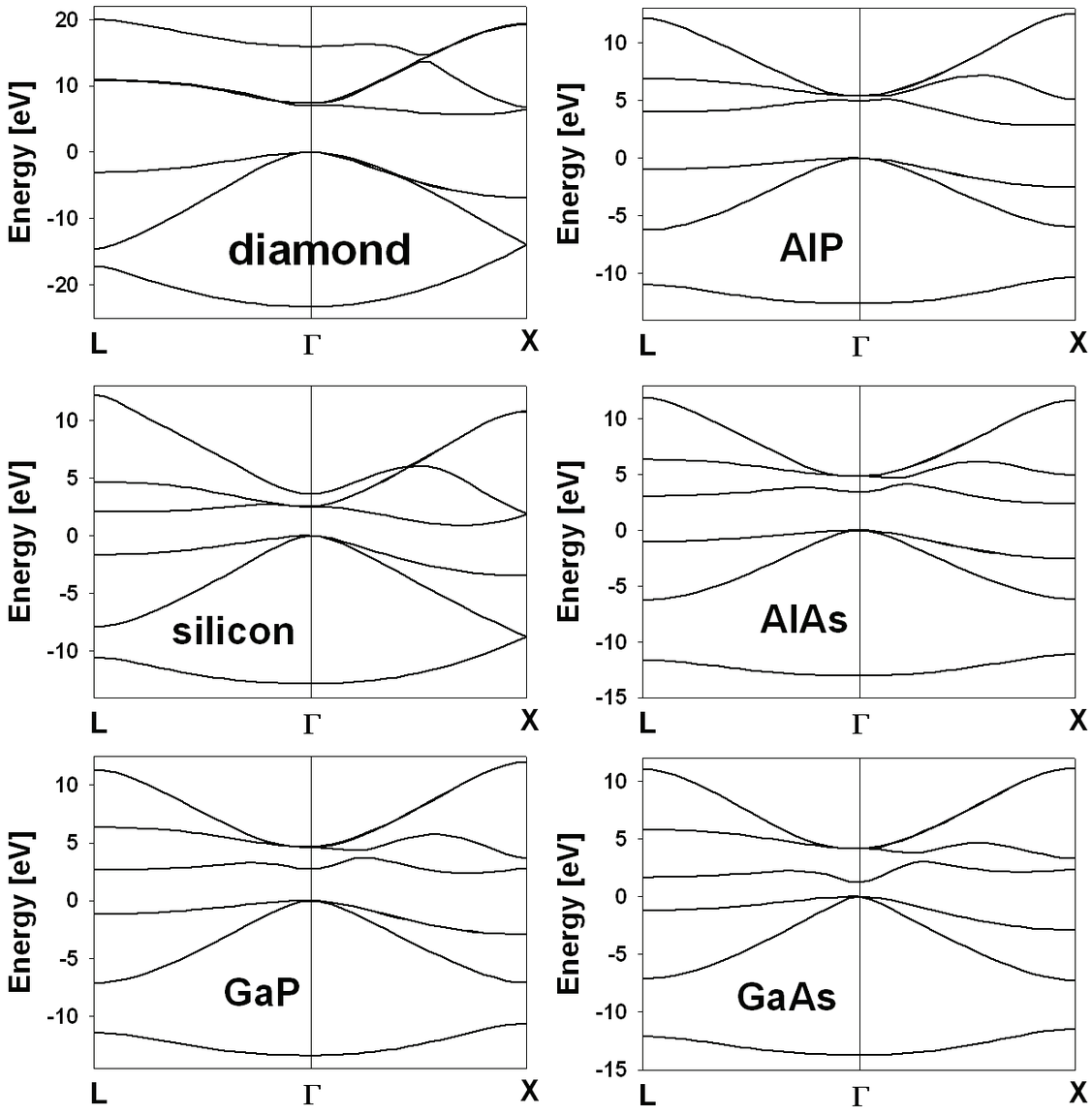

Fig. 2. Energy band structure calculated using eq. (38) with experimental dielectric constant: diamond, silicon, AlP, AlAs, GaP, and GaAs

4.2 Self-consistent calculation for dielectric constant

We summarize the calculation results with the self-consistent dielectric constant, the scheme of which is discussed in Section 2.4, in Table 4. The self-consistent scheme brings in calculation results that are similar to those obtained by using an experimental dielectric constant; for example, eq. (36) based on the self-consistent dielectric constant yields 5.5 eV for the indirect bandgap of diamond, and the use of the experimental dielectric constant yields 5.6 eV.

We demonstrate change of ε_s in the SCF cycle of eq. (36) combined with eq. (39) for diamond in Figure 3. In the figure, we prepare for two different starting (initial) electronic structures; one is the HF electronic structure, and the other is the LDA-SVWN one. In the HF reference calculation, ε_s is underestimated at the early stages of iterative calculations, and then converged to the final value. Conversely, the procedure started from the LDA-SVWN overestimates the dielectric constant at the early stages. There are differences in the initial steps of the self-consistent (SC) cycles, however those dielectric constants are converged to the same value through the iterative calculations. Thus, the same energy band structure is obtained from the SCF cycles even if the initial electronic structures are different. In other words, the self-consistent method does not depend on the starting (initial) electronic structure. On the other hand, the single-shot method, in which the SCF loop is only once calculated, strongly depends on the reference electronic structure. The HF-referenced single-shot calculation underestimates the dielectric constant, $\varepsilon = 2.9$, and it overestimates the bandgap property; the direct and indirect bandgap are 8.5 eV and 6.3 eV, respectively, because the HF method tends to overestimate the bandgap property. On the other hand, the SVWN-referenced single-shot method overestimates the dielectric constant, $\varepsilon_s = 8.1$, and underestimates the bandgap property; the direct and indirect bandgaps are 6.6 eV and 4.4 eV, respectively. Thus, the single-shot calculations yield different results.
Table 5 lists the theoretically determined dielectric constants based on eqs (36), (37), and (38). These calculation results present slight underestimations of the dielectric constant.

		Eq. (36) [eV]	Eq. (37) [eV]	Eq. (38) [eV]
C	Direct	7.0	6.7	6.8
	Indirect	4.9	5.3	5.5
Si	Direct	2.5	2.5	2.6
	Indirect	0.48	0.8	0.95
AlP	Direct	4.9	4.8	4.9
	Indirect	2.0	2.5	2.7
AlAs	Direct	3.5	3.3	3.4
	Indirect	1.5	2.1	2.4
GaP	Direct	2.9	2.8	2.8
	Indirect	2.0	2.3	2.5
GaAs	Direct	1.5	1.3	1.3

Table 4. Bandgaps obtained from the screened HF exchange potential with self-consistent dielectric constant

	Eq. (36)	Eq. (37)	Eq. (38)
C	6.31	6.55	6.51
Si	10.90	11.14	10.83
AlP	8.97	8.69	8.33
AlAs	9.14	8.92	8.58
GaP	8.65	8.87	8.63
GaAs	9.27	9.75	9.55

Table 5. Dielectric constants calculated from self-consistent scheme based on eq. (39)

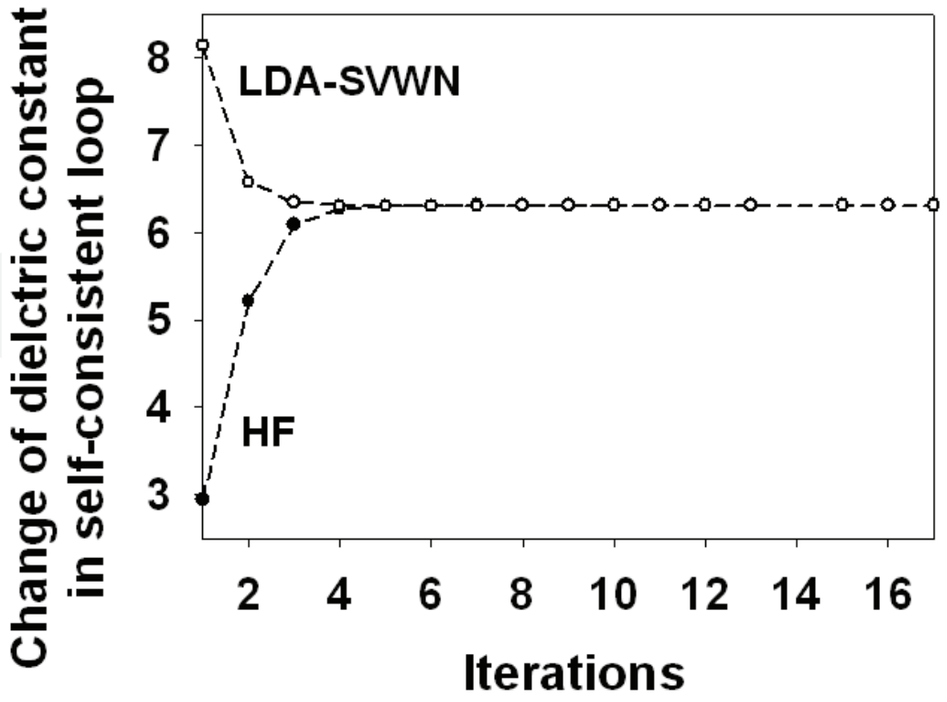

Fig. 3. The change of the dielectric constant in the self-consistent (SC) method for diamond. The black filled circles indicate the SC procedure which starts from the HF energy band structure. The white ones represent the SC procedure started from the LDA-SVWN energy band structure. Two different initials yield the same electronic structure through the iterative procedure. (Shimazaki et al. 2009 b)

5. Discussion

We summarize the inverse of the dielectric constant in Table 1. Those values represent the fraction of the HF exchange term incorporated into the screened HF exchange potential; for example, about 18% and about 8% of the HF exchange terms are used in the screened HF exchange potential for diamond and silicon, respectively. On the other hand, 20% is used for all material in the B3LYP functional. In the case of diamond, the fraction in the proposed method takes a value similar to the fraction in the B3LYP method. However, the HF fraction of the B3LYP functional is larger compared with those of other semiconductors. The B3LYP functional potentially overestimates the bandgap values, other than that of diamond, because a larger fraction of the HF exchange term causes a larger energy bandgap. The HF fraction of the B3LYP functional is set to reproduce the properties of the G1 basis set, which mainly covers light elements such as N, C, and O, and small molecules such as methane, ammonia, and silane.(Curtiss et al. 1990; Pople et al. 1989) Thus, the parameter set of the B3LYP functional is especially suitable for organic molecules. However, the B3LYP functional is not designed for solid-state materials. In order to employ the hybrid-DFT method to solid-state materials, the fraction of the HF exchange term must be decided appropriately.

Here, we emphasize the similarity between the screened HF exchange potential and the hybrid-DFT method. While eqs (37) and (38) are derived from the model dielectric function

of eq. (32) and the local potential approximation, these equations appear to be a type of hybrid-DFT functional. The hybrid-DFT method was introduced by Becke in 1993 by using the adiabatic connection,(Becke 1993 a) and some empirical justifications, such as compensation of the intrinsic self-interaction error (SIE) of semi-local exchange-correlation functional, have been discussed.(Janesko et al. 2009) On the other hand, from the careful observation of actual behaviors of HF and semi-local DFT calculation, the mixing of the HF fraction is reported to bring in useful cancelation, because the semi-local DFT functional have a tendency to overestimate the strength of covalent bonds, and the HF method has the opposite feature.(Janesko et al. 2009) Now, we have proposed an interpretation that the HF fraction represents the incompleteness of the screening effect in semiconductors. Besides, its incompleteness can be described by the inverse of the electronic component of the dielectric constant. This discussion will be helpful to determine an appropriate HF exchange fractions for the target solid-state material.

The screened HF exchange method can be regard as a type of the generalized Kohn-Shan (GKS) method.(Seidl et al. 1996) In the GKS framework, the screened-exchange LDA (sX-LDA) method, which is proposed by Seidl et al., can reproduce eigenvalue gaps in good agreement with experimental bandgaps of several semiconductors. They also presented a calculation result for germanium, employing a semiconductor dielectric function model proposed by Bechstedt et al., and reported that the screening effect of the Bechstedt model is weaker than the Thomas-Fermi model. This feature should correspond to the incompleteness of the screening effect of semiconductors discussed in Section 3.1 because our dielectric function can be derived from a simplification of the Bechstedt model. We should note that the true quasi-particle bandgap is different from the band gap of the GKS method due to the derivative discontinuity of the exchange-correlation potential. However, the discontinuity is, to some extent, incorporated in the GKS single-particle eigenvalues. This fundamental feature of the GKS formalism brings in the improvements of the bandgap calculations of the screened HF exchange method.

Next, we discuss the HSE functional including a splitting parameter ω. The splitting parameter is used to divide the potential into short- and long- range interactions, where the relation of $1/r = erfc(\omega r)/r + erf(\omega r)/r$ is used. The HSE functional has a form similar to our screened HF exchange potential due to the use of $erfc(\omega r)/r$. However, we need to pay attention to the value of ω. In the HSE functional refined by Krukau et al. in 2006, $\omega = 0.11$ is recommended for the parameter.(Krukau et al. 2006) Conversely, in our screened HF exchange potential, the corresponding parameter takes about 0.8. Thus, in the HSE functional, the term of $erfc(\omega r)/r$ can take into account a longer interaction than ours. On the other hand, in our method, the term including $erfc(\omega r)/r$ can represent only short-range interaction because of a large ω value. The long-range interaction in our method is incorporated by the bare HF exchange interaction represented by the second term of eq. (36). The HSE functional has a different theoretical background from our method. Therefore, even if the similar term appears in both methods, the physical meaning is different.

Although the screened HF exchange method and the GW method are taken into account in real space and momentum space, respectively, the both theoretical concepts may be similar, especially in the Coulomb hole plus screened exchange (COHSEX) approximation, because the dielectric function plays an important role in both methods. Gygi et al. have reported that the diagonal-COHSEX approximation has a tendency to underestimate the indirect bandgap property.(Gygi et al. 1986) This feature of diagonal-COHSEX approximation

resembles calculation results determined by eq. (36). The both neglect the energy dependence of the self-energy, and this simplification possibly causes the underestimation of the indirect bandgap property.
In order to describe the screened HF exchange method, we adopt the Gaussian-based formalism; however, our method is not restricted to Gaussian basis sets, and can be used together with other basis set such as the plane-wave basis set. Conversely, the linear muffin-tin orbital (LMTO) and linearized augmented plane wave (LAPW) methods can taken into account the HF exchange term,(Martin 2004) thus our methodology can be easily introduced and implemented in these methods.

6. Summary

This chapter explains the GFT method, which is based on the Gaussian-basis formalism. In the GFT method, the periodic Hartree potential is expanded by auxiliary plane waves, and those expansion coefficients can be calculated by Fourier transform method. We discuss that this simple approach enables us to estimate the Hartree term efficiently. In addition to this, we discuss the screened HF exchange potential, which has a close relationship to the hybrid-DFT method and the GW approximation. In the screened HF exchange potential, the fraction of the HF exchange term is proportional to the inverse of the static dielectric constant, and therefore it depends on the target material. In this chapter, we present not only experimental values but also a self-consistent scheme for the estimation of the dielectric constant. We also discuss that the local potential approximation can expand the possibility of the screened HF exchange method, and it is useful to speculation between the screening effect and the HF fraction term appeared in the hybrid DFT functional.
We have demonstrated the energy band structure of diamond, silicon, AlP, AlAs, GaP, and GaAs from the GFT method and the screened HF exchange potential. The combination of these methodologies can reproduce the experimental bandgap property well. On the other hand, the HF method overestimates the bandgap, while the local DFT (SVWN) method underestimate the bandgap. These kinds of discrepancy between theory and experiment cause the manipulation of the HF exchange term. The fraction of the HF exchange term is closely related to the screening effect, and thus we need to determine the fraction appropriately according to the target system. The discussion in this chapter will be a helpful guideline to determine the fraction.

7. Acknowledgement

This work was partly supported by a Grant-in-Aid for Young Scientists (Start-up) (No. 21850002) from the Japan Society for the Promotion of Science (JSPS).

8. References

Aryasetiawan, F. and O. Gunnarsson. (1998). The GW method, *Rep. Prog. Phys.*, 61, 237-312.

Bechstedt, F., R. D. Sole, G. Cappellini and L. Reining. (1992). AN EFFICIENT METHOD FOR CALCULATING QUASIPARTICLE ENERGIES IN SEMICONDUCTORS, *Solid State Comm.*, 84, 765-770.

Becke, A. D. (1988). Density-functional exchange-energy approximation with correct asymptoic behavior, *Phys. Rev. A*, 38, 3098-3100.

Becke, A. D. (1993 b). Density-functional thermochemistry. III. The role of exact exchange, *J. Chem. Phys.*, 98, 5648-5652.

Becke, A. D. (1993 a). A new mixing of Hartree-Fock and local density-functional theories, *J. Chem. Phys.*, 98, 1372-1377.

Bylander, D. M. and L. Kleinman. (1990). Good semiconductor band gaps with a modified local-density approximation, *Phys. Rev. B*, 41, 7868-7871.

Cappellini, G., R. D. Sole, L. Reining and F. Bechstedt. (1993). Model dielectric function for semiconductors, *Phys. Rev. B*, 47, 9892-9895.

Catti, M., A. Pavese, R. Dovesi and V. R. Saunders. (1993). Static lattice and electron properties of $MgCO_3$ (magnesite) calculated by *ab initio* periodic Hartree-Fock methods, *Phys. Rev. B*, 47, 9189-9198.

Curtiss, L. A., C. Jones, G. W. Trucks, K. Raghavachari and J. A. Pople. (1990). Gaussian-1 theory of molecular energies for second-row compounds, *J. Chem. Phys.*, 93, 2537-2545.

Delhalle, J., L. Piela, J.-L. Bredas and J.-M. Andre. (1980). Multiple expansion in tight-binding Hartree-Fock calculations for infinite model polymers, *Phys. Rev. B*, 22, 6254-6267.

Gygi, F. and A. Baldereschi. (1986). Self-consistent Hartree-Fock and screened-exchange calculations in solids: Application to silicon, *Phys. Rev. B*, 34, 4405-4408(R).

Hedin, L. (1965). New Method for Calculating the One-Particle Green's Function with Applicaton to the Electron-Gas Problem, *Phys. Rev.*, 139, A796-A823.

Heyd, J., G. E. Scuseria and M. Ernzerhof. (2003). Hybrid functionals based on a screened Coulomb potential, *J. Chem. Phys.*, 118, 8207.

Hirata, S. and T. Shimazaki. (2009). Fast second-order many-body perturbation method for extended systems, *Phys. Rev. B*, 80, 085118.

Hirata, S., O. Sode, M. Keceli and T. Shimazaki (2010). Electron correlation in solids: Delocalized and localized orbital approaches, *Accurate Condensed-Phase Quantum Chemistry*, F. R. Manby (Ed.), 129-161, CRC Press, Boca Raton.

Janesko, B. G., T. M. Henderson and G. E. Scuseria. (2009). Screened hybrid density functionals for solid-state chemistry and physics, *Phys. Chem. Chem. Phys.*, 11, 443-454.

Krukau, A. V., O. A. Vydrov, A. F. Izmaylov and G. E. Scuseria. (2006). Influence of the exchange screening parameter on the performance of screened hybrid functionals, *J. Chem. Phys.*, 125, 224106.

Kudin, K. and G. E. Scuseria. (2000). Linear-scaling density-functional theory with Gaussian orbitals and periodic boundary conditions: Efficient evaluation of energy and forces via the fast multipole method, *Phys. Rev. B*, 61, 16440-16453.

Ladik, J. J. (1999). *Phys. Rep.*, 313, 171.

Lee, C., W. Yang and R. G. Parr. (1988). Development of the Colle-Savetti correlation-energy formula into a functional of the electron density, *Phys. Rev. B*, 37, 785-789.

Levine, Z. H. and S. G. Louie. (1982). New model dielectric function and exchange-correlation potential for semiconductors and insulators, *Phys. Rev. B*, 25, 6310-6316.

Martin, R. M. (2004). *Electronic Structure, Basic Theory and Practical Methods*, Cambrige University Press, Cambridge.

Monemar, B. (1973). Fundamental Energy Gaps of AlAs and AlP from Photoluminescence Excitation Spectra, *Phys. Rev. B*, 8, 5711-5718.

Obara, S. and A. Saika. (1986). Efficient recursive computation of molecular integrals over Cartesian Gaussian functions, *J. Chem. Phys.*, 84, 3963-3974.

Parr, R. G. and W. Yang (1994). *Density-functional Theory of Atoms and Molecules*, Oxford Univ. Press, New York.

Penn, D. R. (1962). Wave-Number-Dependent Dielectric Function of Semiconductors, *Phys. Rev.*, 128, 2093-2097.

Piani, C. and R. Dovesi. (1980). Exact-exchange Hartree-Fock calculations for periodic systems. I. Illustration of the method, *Int. J. Quantum Chem.*, 17, 501-516.

Pisani, C., R. Dovesi and C. Roetti (1988). *Hartree-Fock Ab Initio Treatment of Crystalline Systems*, Springer-Verlag, Berlin.

Pople, J. A., M. Head-Gordon, D. J. Fox, K. Raghavachari and L. A. Curtiss. (1989). Gaussian-1 theory: A general procedure for prediction of molecular energies, *J. Chem. Phys.*, 90, 5622-5629.

Seidl, A., A. Görling, P. Vogl, J. A. Majewski and M. Levy. (1996). Generalized Kohn-Sham schemes and the band-gap problem, *Phys. Rev. B*, 53, 3764-3774.

Shimazaki, T. and Y. Asa. (2010). Energy band structure calculations based on screened Hartree–Fock exchange method: Si, AlP, AlAs, GaP, and GaAs, *J. Chem. Phys.*, 132, 224105.

Shimazaki, T. and Y. Asai. (2008). Band structure calculations based on screened Fock exchange method, *Chem. Phys. Lett.*, 466, 91.

Shimazaki, T. and Y. Asai. (2009 a). Electronic Structure Calculations under Periodic Boundary Conditions Based on the Gaussian and Fourier Transform (GFT) Method, *J. Chem. Theory Comput.*, 5, 136-143.

Shimazaki, T. and Y. Asai. (2009 b). First principles band structure calculations based on self-consistent screened Hartree–Fock exchange potential, *J. Chem. Phys.*, 130, 164702.

Shimazaki, T. and S. Hirata. (2009 c). On the Brillouin-Zone Integrations in Second-Order Many-Body Perturbation Calculations for Extended Systems of One-Dimensional Periodicity, *Int. J. Quan. Chem.*, 109, 2953.

Slater, J. C. (1974). *The Self-Consistent Field for Molecules and Solids, Quantum Theory of Molecules and Solids*, McGraw-Hill, New York.

Stevens, W. J., H. Basch and M. Krauss. (1984). Compact effective potentials and efficient shared-exponent basis sets for the first- and second-row atoms, *J. Chem. Phys.*, 81, 6026-6033.

Stevens, W. J., M. Krauss, H. Basch and P. G. Jasien. (1992). Relativistic compact effective potentials and efficient, shared-exponent basis sets for the third-, fourth-, and fifth-row atoms, *Can. J. Chem.*, 70, 612-630.

Vosko, S. H., L. Wilk and M. Nusair. (1980). Accurate spin-dependent electron liquid correlation energies for local spin density calculations: a critical analysis, *Canadian J. Phys.*, 58, 1200-1211.

Yu, P. Y. and M. Cardona (2005). *Fundamental of Semiconductors*, Springer, New York.

Zhu, X. and S. G. Louie. (1991). Quasiparticle band structure of thirteen semiconductors and insulators, *Phys. Rev. B*, 43, 14142-14156.

Ziman, J. M. (1979). *Principles of the Theory of Solids*, Cambridge University Press, Cambridge.

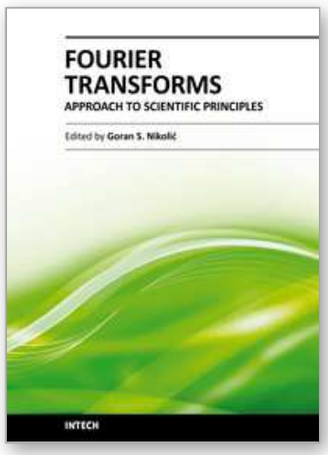

Fourier Transforms - Approach to Scientific Principles
Edited by Prof. Goran Nikolic

ISBN 978-953-307-231-9
Hard cover, 468 pages
Publisher InTech
Published online 11, April, 2011
Published in print edition April, 2011

This book aims to provide information about Fourier transform to those needing to use infrared spectroscopy, by explaining the fundamental aspects of the Fourier transform, and techniques for analyzing infrared data obtained for a wide number of materials. It summarizes the theory, instrumentation, methodology, techniques and application of FTIR spectroscopy, and improves the performance and quality of FTIR spectrophotometers.

InTech Europe
University Campus STeP Ri
Slavka Krautzeka 83/A
51000 Rijeka, Croatia
Phone: +385 (51) 770 447
Fax: +385 (51) 686 166
www.intechopen.com

InTech China
Unit 405, Office Block, Hotel Equatorial Shanghai
No.65, Yan An Road (West), Shanghai, 200040, China
中国上海市延安西路65号上海国际贵都大饭店办公楼405单元
Phone: +86-21-62489820
Fax: +86-21-62489821

IntechOpen